Image-Pair-Based Anisotropic Material Modeling

Jie Feng Wangyu Xiao Bingfeng Zhou *
Institute of Computer Science and Technology, Peking University

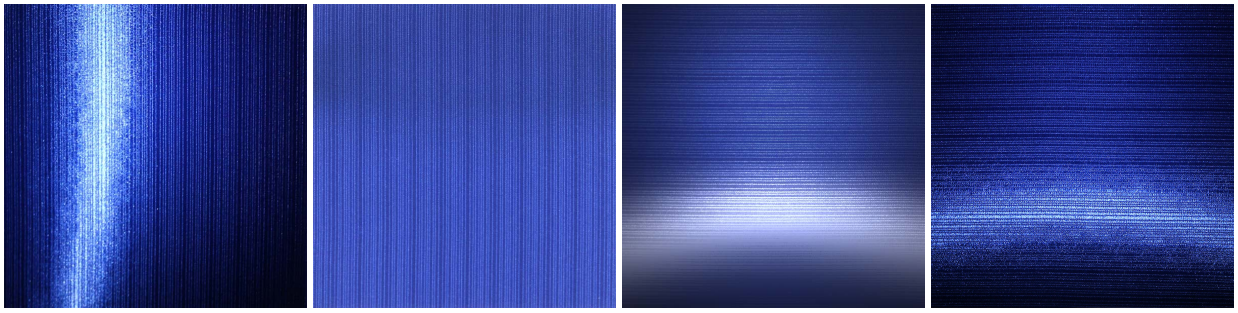

(a) (b) (c) (d)

Figure 1: *Anisotropic material modeling based on a pair of input images: a hightlighted image (a), and a texture image (b). (c) is a rendered image under new viewing conditions using the reflectance and geometry parameters estimated by our method, while (d) is the ground truth image shot under the same viewing conditions with (c).*

Abstract

We present a method for modeling anisotropic materials with only two images taken by an ordinary camera, one under diffuse light which we call *texture image*, and the other under point light named *hightlighted image*. First we decompose the input images into reflectance image and illumination image. Then we use the intrinsic images to obtain the reflectance property and geometry information of the material, including a group of BRDF parameters, an orientation field and a height field. Then images can be rendered with these information under new lighting and viewing conditions.

CR Categories: I.3.3 [Computer Graphics]: Modeling—Rendering

Keywords: image-based material modeling, anisotropy material, image decomposition, orientation field, height field

1 Introduction

Material modeling is important to realistic rendering in computer graphics. It can be realized by measuring BRDF properties. However, measured materials often suffer from large dataset, expensive equipment, and high time consuming. Especially, among all kinds of materials, anisotropic materials have varying appearance with different lighting and viewing directions, and are more difficult in modeling.

In this paper, we present a novel and efficient method for fast anisotropic material modeling. First, the texture and the highlighted image of the material are decomposed respectively into a reflectance image and an illumination image. After that, we use the texture image to calculate the orientation field of the material, and obtain the anisotropic structure of the material. Then we establish an Ashikhmin-Shirley BRDF model, using the illumination component of the highlighted image and the orientation field to solve the model parameters. Finally, we use the model parameters to calculate the height field of the material, which implies the subtle changes in height on the surface of the material. We defines a feature vector for each pixel to measure the distance between pixels, and then, using the k nearest neighbors of each pixel as constraint, a problem of image decomposition is solved to obtain the height field. Using the reflection component of the texture image, orientation field, height field information and the BRDF parameters, we can render new images under different lighting and viewing conditions, hence simulate the realistic material to some extent.

*e-mail:{feng_jie, xiaowangyu, cczbf}@pku.edu.cn. This work is partially supported by NSFC grants #61170206 and #61370112, and the Key Laboratory of Machine Perception (Ministry of Education), Peking University.

SIGGRAPH Asia 2013, November 19 – 22, 2013, Hong Kong.

2 Related work

Image-based material editing modifies the material in a photo to achieve different demands. It needs to acquire the material property or the scene information through limited photos. [Khan et al. 2006] takes a high dynamic range photograph of an object as input and produces as output a new photograph where the object has been given an entirely new material. It does not recover the reflectance property of the object and gives the assumption that surface depth is related to pixel intensity of the image. [Pellacini and Lawrence 2007] edit measured materials and adopt a stroke-based workflow. They use user's strokes as constraints and propagate their property to entire dataset through an optimization that assumes area with similar appearance has similar edits. Our method is inspired by this idea and a feature vector is defined for every pixel and applied to image decomposition and height field estimation.

Image-based material modeling recovers the geometry and the reflectance of objects with multiple images. [Lensch et al. 2001] use a 3D scanner to obtain the object data and generate dense triangle meshes. Then, the reflection property is clustered into several materials. For each material, a BRDF model is fit to the data. However, they need 20-25 HDR images. [Oh et al. 2001] represents a scene as a group of depth images, where each pixel contains both color and depth. It uses a decoupling filter to decouple the illumination

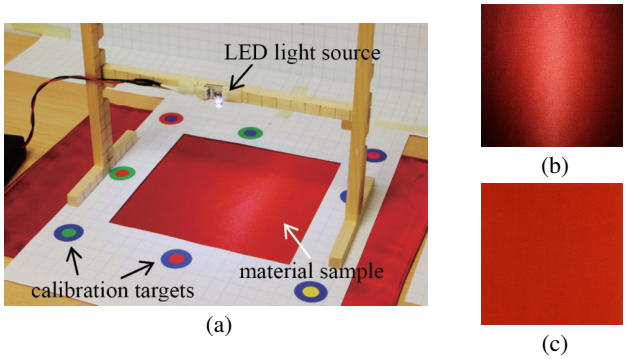

Figure 2: *Image acquiring. (a) The setup of acquiring the highlighted image, (b) the highlighted image and (c) the texture image.*

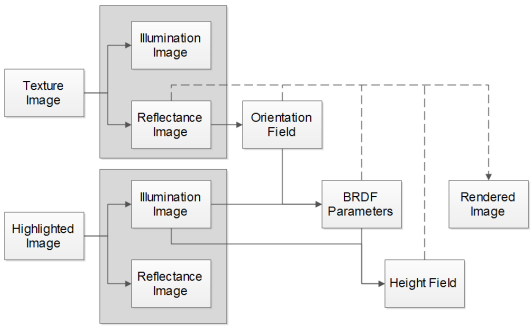

Figure 3: *An overview framework of our method.*

from uniformly textured areas. [Dong et al. 2008] reconstruct a perturbed normal map from the diffuse illumination map and it is insensitive to the light direction. It assigns the specular parameters to each pixel guided by user strokes and the diffuse albedo. In contrast, our method is aimed at obtaining the properties of the material with images as few as possible, and without user assistance.

Decomposing an image into reflectance and illumination is necessary before material analysis. [Tappen et al. 2005] uses color information and a pre-trained classifier to classify reflectance and albedo gradient. [Shen et al. 2008] use non-local texture information as constraints on reflectance between pixels. [Barron and Malik 2012] presents smoothness and minimal entropy priors on albedo, and three priors on shape: the flatness, the orientation of the surface normal near the occluding contour and the variation of mean curvature. Our method gives a different constraint on optimization process and generate better results.

3 Overview

We take as input a highlighted image and a texture image of nearly planar material. The images are taken at the same position. The former (Fig.2(b)) is acquired under a single LED point light source that mounted on a simple scaled stand, as shown in Fig.2(a). The latter is taken under diffuse light as in Fig.2(c). The camera is fixed on a tripod for steady exposure. Its parameters are automatically calculated by a common calibration method with a group of concentric targets printed on the frame around the material sample.

Fig.3 shows the framework of our work. In order to correctly recover the properties of the material, we first decompose respectively the input images into intrinsic images, i.e. a reflectance image and an illumination image. The reflectance component represents the diffuse color of the material, which is invariant to the illumination and viewing conditions; the illumination component encodes the effect of lighting at each pixel. The intrinsic images are used to analyze the corresponding property of the material respectively. Hence the effect of irrelevant component of the input images can be avoided.

Then we utilize the reflectance image of the texture image to calculate the orientation field, which is used with the illumination component of highlighted image to estimate BRDF parameters and height field. Finally, we can render new image under new viewing conditions with the geometry and reflection information.

4 Recovering Intrinsic Images

First, we decompose the highlighted image and the texture image respectively. A *feature vector* is defined for every pixel, which is composed of the pixel color, the average and the standard deviation of the luminance in a 3×3 neighborhood.

The color of pixel (i, j), noted as $I_{i,j}$, is the product of the reflectance $R_{i,j}$ and the illumination $S_{i,j}$, namely:$I(i, j) = R(i, j) \times S(i, j)$. To remove the influence of illumination, we normalize $I_{i,j}$ and $R_{i,j}$, and represent the result as $\hat{I}_{i,j}$and $\hat{R}_{i,j}$ respectively. Let $\hat{R}_{i,j} = \hat{I}_{i,j}$, and now $\hat{R}_{i,j}$ is not the reflectance as it is lacking of intensity component $r_{i,j}$, namely $R_{i,j} = \hat{R}_{i,j} r_{i,j}$. To determine $r_{i,j}$, similar to [Shen et al. 2008], we utilize a Retinex-based method and solve a minimizing problem:

$$\begin{aligned} \min_r \sum_{i,j} [& (\frac{I_{i+1,j}}{\hat{R}_{i+1,j} r_{i+1,j}} - \frac{I_{i,j}}{\hat{R}_{i,j} r_{i,j}})^2 \\ & + (\frac{I_{i,j+1}}{\hat{R}_{i,j+1} r_{i,j+1}} - \frac{I_{i,j}}{\hat{R}_{i,j} r_{i,j}})^2 \\ & + \alpha_{i,j} (\hat{R}_{i+1,j} r_{i+1,j} - \hat{R}_{i,j} r_{i,j})^2 \\ & + \beta_{i,j} (\hat{R}_{i,j+1} r_{i,j+1} - \hat{R}_{i,j} r_{i,j})^2] \\ & + \lambda \sum_i \sum_{j \in N_i} z_{ij} (h_i - h_j)^2, \end{aligned} \tag{1}$$

where,

$$\alpha_{i,j} = \begin{cases} 0.1 & \text{if } |\hat{I}_{i+1,j} - \hat{I}_{i,j}| > 0.01, \\ 10 & \text{otherwise.} \end{cases} \tag{2}$$

$$\beta_{i,j} = \begin{cases} 0.1 & \text{if } |\hat{I}_{i,j+1} - \hat{I}_{i,j}| > 0.01, \\ 10 & \text{otherwise.} \end{cases} \tag{3}$$

In Eq.1, the first two terms penalize large illumination derivatives, while the third and the fourth terms penalize large reflectance derivatives. The fifth term ensures that pixels with similar feature vectors have similar reflectance. N_i is the set of the k nearest neighbors of pixel i, and λ is a constant weight. z_{ij} is the affinity between pixel i and pixel j, namely:

$$z_{ij} = e^{-(\rho_i - \rho_j)^2/2}, \tag{4}$$

where ρ_i and ρ_j are the feature vectors. We optimize this function with L-BFGS method [Nocedal and Wright 2006] and use kd-tree to provide fast retrieval. Fig.4 shows a comparision with [Dong et al. 2008]. Notice that there are obvious shading in reflection image (b) and white lines in bottom right in illumination image (c), while in our result these artifacts are removed.

5 Recovering Geometry and Reflection

5.1 Calculating Orientation Field

The fine-line textures shown on anisotropic materials are determined by their microstructures. According to the Ashikhmin-

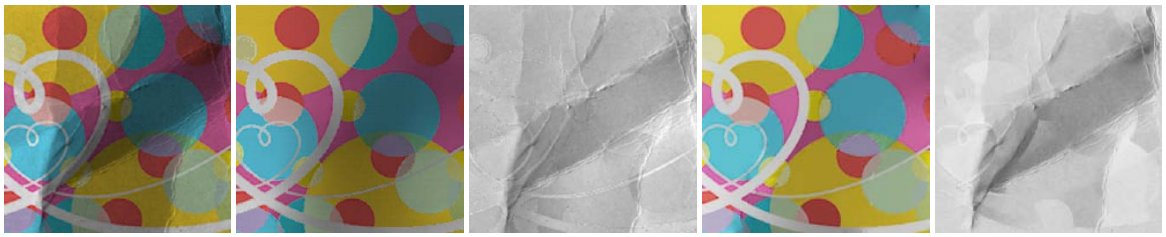

(a) (b) (c) (d) (e)

Figure 4: *Result of image decomposition. (a) is the input image, (b) and (c) are the reflection image and the illumination image respectively before user-assisted refinement in [Dong et al. 2008], (d) and (e) are our result.*

Shirley model [Ashikhmin and Shirley 2000], anisotropic reflectance features are directly related to such facet distribution. Therefore, capturing the orientation field of the fine-lines is the first step of reflectance modeling.

The methods in [Paris et al. 2004; Holroyd et al. 2008] require multiple input images taken with varying light sources. Instead, here we adopt a simpler method and extract orientation field from a single input texture image. First, an initial orientation field is calculated based on the image gradient. For each pixel, its orientation angle is formulated as:

$$\theta_{ij} = \arctan(\frac{I_y(i,j)}{I_x(i,j)}) + \frac{\pi}{2}, \tag{5}$$

where $(I_x(i,j), I_y(i,j))$ is the gradient vector on position (i,j), calculated by a pair of Sobel operators. The result of Eq.5 may include a lot of noise as shown in Fig.5(b), so we segment the image into patches to get stable orientation field. The dominant orientation [Rao and Schunck 1989] of an $s \times t$ patch is defined as:

$$\theta_p = \frac{1}{2}\arctan(\frac{\sum_{i=1}^{s}\sum_{j=1}^{t} 2I_x(i,j)I_y(i,j)}{\sum_{i=1}^{s}\sum_{j=1}^{t} I_x^2(i,j)I_y^2(i,j)}) + \frac{\pi}{2}, \tag{6}$$

and a patch coherence k_p is calculated as following to measure its fitting error:

$$k_p = \frac{\sum_{i=1}^{s}\sum_{j=1}^{t} |I_x(i,j)\cos\theta_p + I_y(i,j)\sin\theta_p|}{\sum_{i=1}^{s}\sum_{j=1}^{t}\sqrt{I_x^2(i,j)I_y^2(i,j)}}. \tag{7}$$

Then, an iterative optimizing procedure is performed to remove noise. The patches with poor orientation coherence ($k_p < 0.4$) are marked as invalid. For each invalid patch, if there are at least 4 valid patches in its 8-neighborhood, its dominant orientation angle is recalculated according to the *N* valid neighbors:

$$\theta_p' = \frac{1}{2}\arctan(\frac{\sum_{i=1}^{N}\sin 2\theta_i}{\sum_{i=1}^{N}\cos 2\theta_i}). \tag{8}$$

This step will be repeated until all patches become valid. After that, we further perform an inter-patch smoothing so that more isolated noises can be filtered out. A neighborhood coherence k_n is calculated for each patch with its neighbors' dominant angles, in the same way as in Eq.7. If k_n is smaller than a threshold, the angle of current patch is recalculated again with Eq.8.

An optimized orientation field is shown in Fig.5(c). The short slashes indicate dominant angles of each 7×7 patch. We can find that most of the wrong patch orientations have been corrected. Finally, in the whole image, each pixel's orientation angle θ_{ij}' is updated by bilinear interpolating according to its 4 nearest patches' dominant angles. Therefore, we can obtain a smooth and continuous orientation field as shown in Fig.5(d), which is illustrated in a hue map.

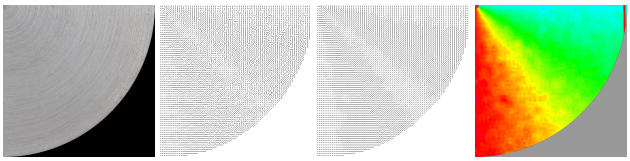

(a) (b) (c) (d)

Figure 5: *Calculating orientation field from a single image. (a) Texture image; (b) Initial orientation field (patched); (c) Optimized orientation field; (d) Interpolated continuous orientation field.*

5.2 Estimating Anisotropic BRDF Parameters

To estimate the reflection property of the material, we adopt Ashikhmin-Shirley BRDF model, where there are four parameters: n_u and n_v that control the shape of the reflectance lobe; the diffuse and the specular coefficients, R_d and R_s. We obtain the parameters by solving the following problem:

$$\min(1 - ssim(I(R_s, R_d, n_u, n_v), I_0)), \tag{9}$$

Here, $I(R_s, R_d, n_u, n_v)$ is the image rendered with the parameters, and I_0 is the illumination image decomposed from the input highlighted image; $ssim(I, I_0)$ represents the structural similarity [Wang et al. 2004] of the rendered image and the shading image.

Two groups of rendering results with the estimated parameters are given in Fig.6. We can see that the rendered illumination images are close to the real images in appearance.

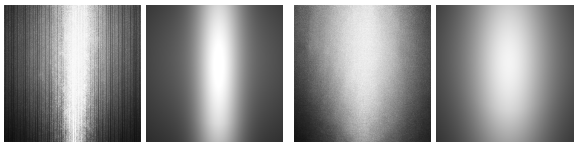

Figure 6: *Parameter estimating results for two examples. For each example, Left: illumination component of the highlighted image; Right: rendered image with estimated BRDF parameters.*

5.3 Computing Height Field

From Fig.6, we can see that the rendered images have similar appearance in illumination with the input image, but lack of some texture details. Although the material is almost flat, there still exists slight difference in height in the surface. To obtain better rendering result, we further estimate a height field of the material through the Ashikhmin-Shirley BRDF model again.

We also define a *feature vector* for each pixel, which has 3 dimensions: the luminance, the gradient along x and y direction. We assume that pixels with similar feature vectors have similar height.

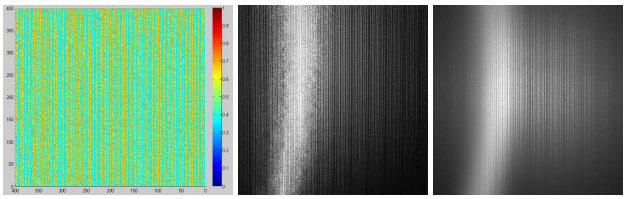

(a) (b) (c)

Figure 7: *Rendered result using the estimated height field. (a) The estimated hight field of Fig.1(b); (b) The ground truth image; (c) The rendered illumination image.*

Hence, the height field can be calculated by formulating an optimization problem as follows:

$$\min_{H} MSE(I(H) - I') + \lambda \sum_{i} \sum_{j \in N_i} z_{ij}(h_i - h_j)^2, \qquad (10)$$

where I' is the illumination image and $I(H)$ is the rendered image using the height field and the parameters from section 5.2, λ is a constant weight and N_i represents the nearest pixels of pixel i. The definition of z_{ij} is the same as Eq.4.

We initialize the height field with the gray value of the input texture image and then solve the problem using L-BFGS method. Fig.7 shows a rendering result using the estimated height field, in which the texture details are properly reconstructed, and the rendered image is more realistic than the results in Fig.6.

6 Experimental Results

With the estimated BRDF parameters and the orientation/height field, we can render the material under new viewing conditions by combining the synthesized illumination image and the reflectance component of the texture image. For the blue silk material, whose input image pair is given in Fig.1 (a) and (b), Fig.1(c) show its rendering result in a new viewing direction. More rendering results and the comparison with the ground truth image are given in Fig.8.

7 Conclusions and Future Work

In this paper, we propose an efficient anisotropic material modeling method that requires only one image pair and no expensive equipments. The simplicity provides the method many potential applications, especially where quick and inexpensive material approximation is needed.

However, current method works only on nearly planar materials. The pixel normal is simply assumed to be upward. In the future work, we will reconstruct a spacial-variance normal distribution so that the rendering results will be improved. Our gradient-based method should also be improved to increase the reliability of the orientation field. Furthermore, the method can be extended to model inhomogeneous materials.

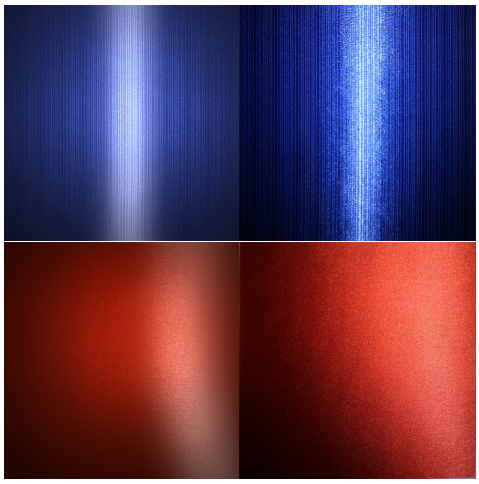

Figure 8: *Rendering results under new viewing conditions. Upper: rendering result from Fig.1(a) and (b); Lower: rendering result from Fig.2(b) and (c). For each group, Left: the rendered image; Right: the ground truth image.*

References

ASHIKHMIN, M., AND SHIRLEY, P. 2000. An Anisotropic Phong BRDF Model. 25–32.

BARRON, J. T., AND MALIK, J. 2012. Shape, Albedo, and Illumination from a Single Image of an Unknown Object. *CVPR*.

DONG, Y., TONG, X., PELLACINI, F., AND GUO, B. 2008. AppGen: interactive material modeling from a single image. *ACM Transactions on Graphics*, 1–10.

HOLROYD, M., LAWRENCE, J., HUMPHREYS, G., AND ZICKLER, T. 2008. A photometric approach for estimating normals and tangents. *ACM Transactions on Graphics 27*.

KHAN, E. A., REINHARD, E., FLEMING, R. W., AND BLTHOFF, H. H. 2006. Image-based material editing. *ACM Transactions on Graphics 25*, 654–663.

LENSCH, H. P. A., GOESELE, M., KAUTZ, J., HEIDRICH, W., AND PETER SEIDEL, H. 2001. Image-Based Reconstruction of Spatially Varying Materials. In *Eurographics Symposium on Rendering/Eurographics Workshop on Rendering Techniques*, 103–114.

NOCEDAL, J., AND WRIGHT, S. J. 2006. *Numerical Optimization*. Springer.

OH, B. M., CHEN, M., DORSEY, J., AND DURAND, F. 2001. Image-based modeling and photo editing. In *Annual Conference on Computer Graphics*, 433–442.

PARIS, S., BRICEO, H. M., AND SILLION, F. X. 2004. Capture of hair geometry from multiple images. *ACM Transactions on Graphics 23*, 712–719.

PELLACINI, F., AND LAWRENCE, J. 2007. AppWand: editing measured materials using appearance-driven optimization. *ACM Transactions on Graphics 26*.

RAO, A. R., AND SCHUNCK, B. G. 1989. Computing oriented texture fields. In *Computer Vision and Pattern Recognition*, 61–68.

SHEN, L., TAN, P., AND LIN, S. 2008. Intrinsic image decomposition with non-local texture cues. In *Computer Vision and Pattern Recognition*, 1–7.

TAPPEN, M. F., FREEMAN, W. T., AND ADELSON, E. H. 2005. Recovering Intrinsic Images from a Single Image. *IEEE Transactions on Pattern Analysis and Machine Intelligence 27*, 1459–1472.

WANG, Z., BOVIK, A. C., SHEIKH, H. R., AND SIMONCELLI, E. P. 2004. Image quality assessment: from error visibility to structural similarity. *IEEE Transactions on Image Processing 13*, 600–612.